Nitrate Electrochemical Reduction using Modified Boron Doped Diamond Electrode from Copper Electroless

Abstract

Modified boron doped diamond (BDD) electrodes from copper (Cu) electroless process were produced and characterized aiming their application on nitrate electrochemical removal. Cu particles may promoted BDD conductivity as well as its selectivity increase in the nitrate ions reduction using the flow electrochemical reactor. Cu/BDD composites were obtained with optimized parameters to produce high quality electrodes in suitable doping level and Cu particle deposits. BDD films were grown on titanium (Ti) substrates from hot filament chemical vapor deposition reactor. A higher deposit density as well as a better Cu particles uniformity were observed for higher doped BDD electrodes. Considering the nitrate reduction, four cathode and four anode electrodes with 2.5 x 2.5 cm^2 were necessary for each electrolysis. The experiments were carried out by varying current density, reactor flow rate, and supporting electrolyte. The process effectiveness was analyzed as a function of BDD/Ti and/or Cu/BDD/Ti electrodes as cathode. The electrolysis efficiency was analyzed by Ion Cromatography. Preliminary results showed that the highest electrolysis efficiency for flow rates of 300 L h^{-1} when BDD/Ti electrodes were used in both as anode and as cathode simultaneously. These results were corroborated by X-ray photoelectron spectroscopy (XPS) measurements for electrode surfaces before and after the electrolysis. This behavior may be associated to the lower impurity adsorption on the film surface due to the turbulent flow reactor. On the other hand, when Cu/BDD/Ti was used as cathode, the best efficiency was obtained for flow rate of 50 L h^{-1}, which may be associated to the low hydrogen adsorption on the electrode surface due to the Cu presence.

Keywords: Electroless, copper, nitrate reduction, reactor.

1. Introduction

The quality of drinking water in the world has been directly affected by anthropogenic factors [1]. In addition to the problem of the availability of potable water, there is the issue of pollution by wastewater discarded from households, commercial establishments, and industries through sanitary sewers. It is possible to observe the impacts generated by the contamination of water resources throughout in society as well as in public health [2], affecting mainly the places where water does not receive any type of treatment. Among the materials found as contaminants of groundwater source, nitrate ion can cause a significant environmental problem. It is generated due to the use of fertilizer products containing large concentrations of nitrogen compounds in addition to inorganic and animal manure, in plantations, soil cultivation, sewage deposited in septic systems, and atmospheric deposition [3]. A recent concern is the increase of nitrate ion levels in drinking water. Particularly in healthy water in rural areas, the main

source of this nitrate is caused by leaching out of cultivated land to rivers and water streams, which can contaminate large areas [4]. The consumption of high concentrations of nitrate ion through the supply water is associated with two adverse health effects: induction to methemoglobinemia [5] and the potential formation of carcinogenic nitrosamines and nitrosamides [6]. Diseases related to the lack of water treatment are a reality, thus, in order to solve these problems, many works have been developed to improve the quality of water in lakes, rivers, aquifers and management as discussed in an analysis between the Brazilian circumstance and the world water development [7].

There are different studies that attempt to remove nitrate from water, which use different techniques such as: biological treatment [8], ion exchange [9], reverse osmosis [10], heterogeneous catalysis [11], and electrochemistry [12-15]. Among them, electrochemical technology has been shown to be an excellent nitrate removal technique because it has advantages such as: relatively low cost, safe technique, small areas for plant implantation, and being environmentally correct due to the use of electron exchange in the electrochemical reduction/oxidation process. It is important to point out that this technique is strongly influenced by the type of electrode, type of catalyst, pH, and hydrogen flow rate [4]. Concerning the electrochemically-induced nitrate reduction, cathode material is determinant in this technology efficiency and many metals have been already studied as cathodes like Cu, Fe, Al, Ni, Zn, Ag, Au, Pt and Pd [16-20]. Among them, Cu and Fe have demonstrated to be the very promise associated to their high efficiency and low cost.

In addition, boron doped diamond (BDD) has been extensively used as electrode material due to its peculiar properties including the wide potential window, allowing the work in cathodic and anodic region extremes, corrosion resistance, high electrical and thermal conductivity, low background current, and high chemical inertia [21], particularly with high efficiency for nitrates removal [22-25]. Recently, Rajic et. al. [4] have discussed the complex process concern to the electro-reduction of nitrate at the cathode which starts with nitrate ion absorption. In similar way, Kalaruban et. al. [9] have shown the possible reactions at the cathode and at the anode where the oxygen evolution is the main anodic reaction. By using a undivided electrolytic cell, Govindan et al. [26] have studied the mechanism for nitrate removal where nitrite and ammonia are the main products formed during the electrochemical process. They explained the understanding of this mechanism associated to the formation of ammonia from nitrate and nitrite at cathode and subsequent re-oxidation of ammonia to nitrogen on the catalytic anode surfaces. Their results followed the same trend as discussed by Perez et al. [21] by using BDD electrodes in the absence of chloride ions.

Also, we have already studied in previous paper the reactions that may occur anodically on BDD electrode enhancing the $^{\bullet}OH$ production [27]. Following this reaction, we can supposed that at the beginning of electrolysis the low NH_4^+ formation may be due to the high quantity of hydroxyl radicals generated on BDD anode, which facilitates the direct ammonia oxidation to nitrogen gas. This assumption is consistent with that reported by Ghazouani et al. [28]. According to them, the hydroxyl radicals are rapidly produced on BDD anode and reach a maximum after 30 min, then, decreases up to the end of electrolysis.

Taking into account the above discussions as well as our previous optimized study in the production and characterization of Cu/BDD/Ti electrodes at different experimental parameters [29], this manuscript shows the application of these electrodes for nitrate removal using the flow electrochemical reactor. From these previous results concerning the Cu deposits on BDD surface, we chosen the best Cu/BDD/Ti electrode taking into account the electroless parameter variations for two different BDD doping

levels, at three pH solutions, and at three deposition times. Thus, we discuss the nitrate electrochemical reduction improvement using two sets of BDD/Ti as anodo and BDD/Ti or Cu/BDD/Ti electrodes as cathode in the electrochemical flow reactor, at different current densities, flow rates, and different supporting electrolyte. The electrolysis results were monitored by ion chromatography technique.

2. Experimental

2.1. Cu/BDD/Ti production and characterization

Firstly, as already described in previous work [29] to optimize the parameters for Cu/BDD/Ti production from electroless process, BDD films were grown on Ti substrates with geometric area of 1.0 x 1.0 cm^2 and thickness of 0.5 mm by hot filament chemical vapor deposition (HFCVD) technique. To minimize the stress film/substrate and to increase the nucleation rate BDD coatings were deposited on Ti after pre-treatment in air abrasion with glass beads. They were prepared from methane hydrogen gas mixture with a pressure of 40 Torr and temperature around 650ºC for 24 h. Boron source was obtained by an additional hydrogen line passing through a bubbler containing B_2O_3 dissolved in methanol with a controlled B/C ratio that permitted to produce films with different doping levels (5000 and 15000 ppm B/C). To estimate the B acceptor density for the heavily BDD sample, Mott-Schottky plots (MSP) curves were taken in 0.5 mol L^{-1} H_2SO_4 for frequency of 10 kHz, peak to peak potential perturbation of 10 mV, and potential range from 0 to 1.0 V x Ag/AgCl/KCl(sat). Prior to the Cu electroless deposition, the sensitization on the BDD was achieved using a solution of 40 mL L^{-1} HCl containing 0.04 mol L^{-1} $SnCl_2$ for 5 min and the activation was made using a solution containing $7x10^{-4}$ mol L^{-1} $PdCl_2$ with 2.5 mL L^{-1} HCl for 5 min. Ultrasonic vibration was used for both steps. The electroless Cu deposition was carried out for different times (30, 60, 180 and 2400 s) at room temperature. The bath composition was 0.1 mol L^{-1} $CuSO_4$ + 0.2 mol L^{-1} $KNaC_4H_4O_6$ + 17.5 mL L^{-1} HCHO. The pH level was adjusted to 8, 10 and 12 by the addition of NaOH. Fourier transform infrared (FTIR) spectrometer with attenuated total reflectance (ATR) Model Spectrum 100 from Parkin Elmer equipment was used to monitor the anchor points associated with the functional groups on BDD surfaces promoted by the pre-treatments. The Cu modified diamond films morphology was verified from the scanning electron microscopy (SEM) images using a Jeol JSM-5310 microscope and the X-ray Diffraction (XRD) patterns using a PAN analytical model X'Pert Powder diffractometer with the CuKα (λ = 1.54 Å), set at 45 kV and 25 mA, running in the ω/2θ scanning mode with ω = 1° and 2θ from 10 to100°. These morphological and structural characterizations were already described in details in our previous paper [29].

Therefore, after the parameter optimizations in this Cu electroless process to produce Cu/BDD/Ti electrodes, for electrochemical responses BDD/Ti films were grown on Ti with geometric area of 2.5 x 2.5 cm^2 and thickness of 1.5 mm following the same experimental procedures, but only in the highest doping level of 15000 ppm B/C. For these samples, the Cu electroless parameters were optimized as solution pH = 12 and deposition time of 30 s. The best electrode performance was also confirmed by linear sweep voltammetry (LSV) measurements for nitrate reduction using 1 mmol L^{-1} Britton-Robinson (BR) buffer (pH=3) + 0,01 mol L^{-1} KNO_3 at sweeping rate of 50 mVs^{-1} for /CuBDD/Ti electrodes at deposition times of 30 ,60, and 180 s. LSV and MSP experiments were taken using a conventional electrochemical cell and a Potentiost/Galvanostat 302 Autolab/Metrohn equipment with Pt as counter and Ag/AgCl/$KCl_{(sat)}$ as reference electrodes, respectively.

2.2. Nitrate reduction using the electroctrochemical flow reator

Taking into account the electrochemical nitrate reduction the electrolysis were performed using a adapted and assembled electrochemical flow reactor from a previous work according to Fig.1 [30]. This reactor comprising two parallel polypropylene plates fitted with four electrodes as anodes (total geometric area 16.6 cm^2) and four electrodes as cathodes (total geometric area 16.6 cm^2). The reactor was connected to a recirculation system (capacity 2.0 L) through which electrolyte could be supplied at flow rates from 50 L h^{-1} (laminar flow; Re 300) to 300 L h^{-1} (turbulent flow; Re 1900). The experiments were carried out using four BDD/Ti electrodes as anode and four BDD/Ti or Cu/BDD/Ti as cathode using 800 mL of nitrate solution and electrolysis time for 5 h. Aliquots were taken at times: 0, 15, 30, 45, 60, 75, 90, 105, 120, 150, 180, 210, 240, 270 e 300 min. They were analyzed using a Ion Cromatography 850 Profissional Metrhom system with an anions column Metrosep A supp 5 and eluent of 0,003 mol L^{-1} Na_2CO_3 + 0.001 mol L^{-1} $NaHCO_3$. For all experiments the distance between the anodes and cathodes was kept constant at 1.5 cm.

Firstly we carried out the electrolysis in neutral solution 0.1 mol L^{-1} de K_2SO_4 + 100 ppm de KNO_3 using BDD/Ti electrodes as cathodes and anodes at two current densities of 20 and 200 mA cm^{-2} for three different flow rates of 50, 100, and 300 L h^{-1}. Secondly, from the best current density value, the electrolysis were performed using Cu/BDD/Ti as cathodes and BDD/Ti as anodes for two different flow rates of 50 and and 300 L h^{-1}. Following the late configuration of the electrodes it was also studied the influence of supporting electrolyte for nitrate removal. For comparison, the electrolysis were performed a second solution of 0.1 mol L^{-1} phosphate buffer solution (pH=7) + 100 ppm KNO_3 and a third solution of 0.1 mol L^{-1} carbonate buffer solution (pH=10) + 100 ppm KNO_3. After each electrolysis process the electrodes were rinsed with isopropyl alcohol in ultrasound bath. Finally, to evaluate the chemical adsorption on the electrode surfaces after the electrolysis process, the electrode chemical compositions were analyzed from X-ray photoelectron spectroscopy (XPS) measurements using a Kratos Axis Ultra XPS system with X-ray Al-Kα (λ = 1486.5 eV).

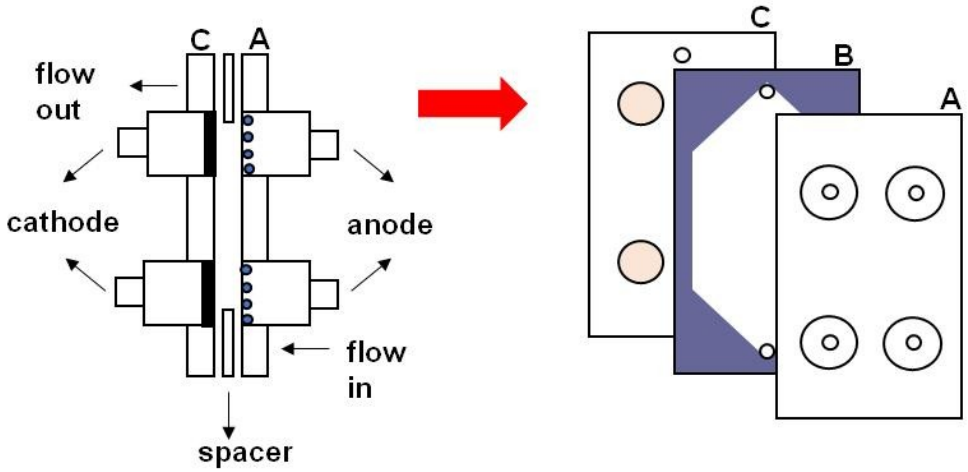

Figure 1.Schematic view of the electrochemical flow reactor. A,B, and C represent the external, spacer, and internal parts, respectively.

3. Results and Discussions

3.1. Characterization of BDD/Ti and Cu/BDD/Ti electrodes

The results of the morphological and structural characterizations of the electrodes used in this paper, through scanning electron microscopy (SEM), Raman spectroscopy, X-ray spectra, and Fourier Transformer Infrared spectroscopy (FTIR) analyzes have previously been presented [29]. BDD films completely closed and homogeneous were observed covering the entire substrate considering their roughness morphology. The films did not present cracks or delaminations even after electrolysis experiments. Raman spectra showed high quality BDD films for both doping levels confirmed by the diamond peak presence in the region of 1332 cm^{-1}. The physical meaning of a MSP is the effect of potential E on the thickness of the space-charge layer in the semiconductor. The MSP was used to obtain the boron content on BDD films obtained with different doping levels. Fig 2 depicts this graph for the heavily BDD sample (15000 ppm B/C), with a classical Mott-Schottky behavior and weak frequency dependence, where the slope of the curve allows to determine its acceptor density. The evaluated acceptor density value is 2.42 x 10^{21} $B.cm^{-3}$, indicating a heavy doped film with an excellent conductivity and very suitable for electrochemical applications confirming its profile presented in Raman analyses. Concerning the Cu electroless process, the deposits presented small grains morphology distributed all over the diamond crystal faces for both electrodes depend on the electrode boron level, solution pH, and deposition time. Cu metallic crystallographic form was obtained for all depositions. The deposits increased with increasing the pH solution as well as the deposition time. SEM images showed high density of Cu particles for the highest doped BDD electrode. Therefore, from the optimized electroless parameters, we chosen the Cu/BDD/Ti electrodes obtained with pH =12, with the highest doping level, evaluated from Mott-Schottky Plot (MSP), as described above.

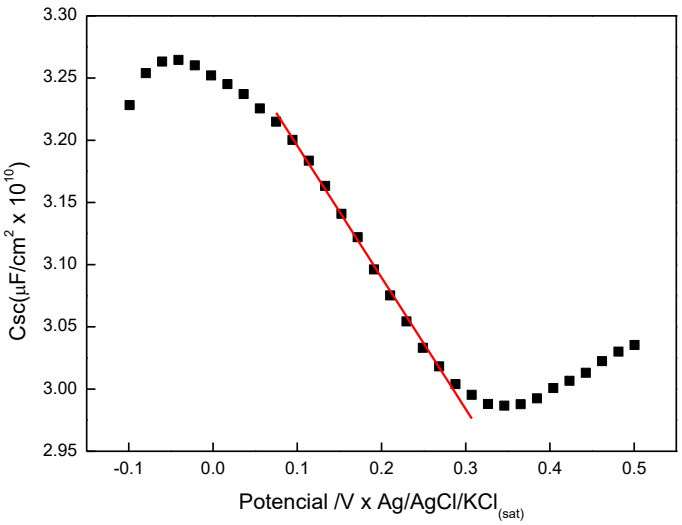

Figure 2. MSP curve for the heavily BDD/Ti sample.

The modified Cu/BDD/Ti electrodes at different deposition times were used to evaluate their performance to the nitrate reduction. This analysis was carried out with the purpose of choosing which time of deposition presented the greatest performance with respect to the activity and selectivity in the nitrate eletroreduction. This result was important because the best response obtained in this measurement was used as a definition parameter in the electroless deposition time applied to the larger electrodes, which were used in the electrochemical flow reactor Fig. 3 presents linear sweep voltamograms of these electrodes in the presence of nitrate ion as a function of Cu deposition time. For comparison the curve D is related to the Cu/BDD/Ti - 30 s only on BR buffer solution (blank). It is possible to observe that Cu deposited on diamond surface catalyse the electroreduction of nitrate for all electrodes. Nitrate electroreduction is a very complex process. Several products are possible depending on the experimental conditions such as pH and applied potential. In this work, the cathodic peak is observed around -0.6 V x $Ag/AgCl/KCl_{(sat)}$ for the three electrodes studied , suggesting that nitrate to nitrite reduction is taking place at this potential.

As can be observed in Fig. 3(C), despite the high density of Cu particles deposited on the BDD surface with deposition time of 180s (C) [29], did not increase the catalytic activity for nitrate reduction, since the voltamogram of the nitrate showed a lower cathodic current when compared to those of Cu/BDD/Ti obtained at deposition times of 30 (A) and 60s (B). A more significant difference was observed in the voltammogram of the Cu/BDD/Ti electrode of 30s deposition time (A), which showed a peak around -0.6 V x $Ag/AgCl/KCl_{(sat)}$ related to nitrate to nitrite reduction followed by a shoulder around -1.1 V x $Ag/AgCl/KCl_{(sat)}$ relative to the nitrate reduction to ammonia. In addition, a slight increase in cathodic current is observed, showing that the reduction of nitrate was better catalyzed in the presence of smaller amounts of Cu particles. Therefore, Cu/BDD/Ti-30s electrode presented the better activity and selectivity for both nitrite and ammonia ions in nitrate reduction while Cu/BDD/Ti electrodes obtained at 60 and 180 s deposition times presented activity and selectivity only for nitrite ion. However, it is important to note that the Cu/BDD/Ti-60s showed the largest peak definition related to nitrate to nitrite reduction. Thus, the deposition time of 30 s was chosen for Cu electroless process on larger BDD electrode (2.5 x 2.5 cm^2) for using in nitrate removal in the electrochemical flow reactor.

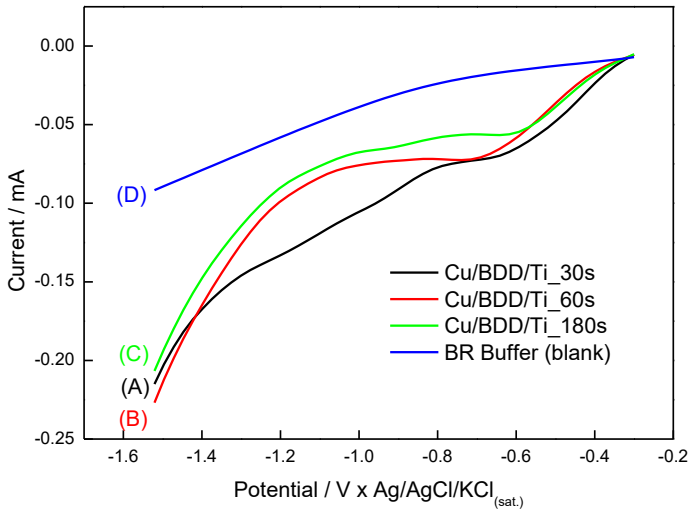

Figure 3. LSV response of Cu/BDD/Ti electrodes with deposition times of 30, 60 and 180 s for 10^{-3} mol L^{-1} BR buffer solutions (pH=3) and for nitrate reduction in solution of 10^{-2} mol L^{-1} KNO_3 + 10^{-3} mol L^{-1} BR buffer solution (pH=3). Scan rate: 50 mV s^{-1}.

3.2. Electrolysis of nitrate ions

The study for nitrate removal was performed in a systematic way considering different experimental parameters on the electrochemical flow reactor. Firstly, some criteria were established to impose a range for these parameter variations. Concerning the supporting electrolyte, it was chosen to fix the neutral medium of K_2SO_4 due to its same cation of the reagent KNO_3 decreasing in this way the amount of ions and, consequently, decreasing the probability of peak overlaps for ion chromatography analyses. We chose two values of current density 20 and 200 mAcm^{-2}. The minimum current value is explained by the mass transfer model used to estimate the minimum necessary current to degrade nitrate to obtain nitrite and ammonium as final products [14,15]. Besides, other studies have already discussed the nitrate degradation efficiency in this current range [14, 15, 31]. On the other range, the second current value was chosen due to studies that have reported good degradation results with higher current values [32, 33], and also attributed to our interest to investigate the behavior of degradation that uses, comparatively, a current ten times greater. Thus, two values of current density, different in one order of magnitude, were defined to investigate a possible proportionality relationship between the current density and the percentage of degraded nitrate.

3.2.1. Influence of flow rate and current density

For this purpose the reactor set up was kept using BDD/Ti electrodes for anodes and for cathodes where three flow rates of 50, 100, and 300 L h^{-1} were studied in the two current densities of 20 and 200 mA cm^{-2}. For the experiments using 20 mA cm^{-2} the electrolysis results are presented in Fig. 4(a) where for all flow rate showed the degradation of part of the pollutant, implying a sharp decrease in the nitrate concentration at the beginning of the experiments, even though this decay rate did not show continuity after the first hour of degradation. Indeed, on the cathode surface there is a competition between the nitrate and the hydrogen reduction. Thus, it is believed that the degradation rate was reduced after the first hour due to the physical adsorption of the hydrogen on the electrode surface, decreasing the interaction between the electrode and the pollutant over time not to mention the possible adsorption of intermediate compounds generated during the degradation. As explained in the experimental part, aliquots were taken during the electrolysis process and the results were analyzed by ion chromatography. The obtained values were normalized in all the presented results. The electrolysis of the pollutant at the fluxes of 50 (A) and 100 L h^{-1} (B) were very similar, with nitrate removal of 6 and 7%, respectively. On the other hand, in the flow rate of 300 L (C) h^{-1} the degradation was greater, reducing 13% of the pollutant. As the nitrate reduction values were very closer for flow rates of 50 and 100 L h^{-1} it is possible to speculate that the small variation in flow rate was not sufficient to change the laminar flow regime established in the smaller flow rates. In contrast to this result, the significant nitrate removal increase in the flow rate of 300 L h^{-1} was attributed to the lower adsorption of hydrogen particles and/or intermediate products on the electrode surfaces provided by its turbulent fluid flow regime. Considering the nitrate removal

experiments for 200 mAcm^{-2}, similar results were observed for the flows of 50 (A) and 100 L h^{-1} (B) of 11 and 12%, respectively. Following the same degradation behavior performed at 20 mA cm^{-2}, the best response occurred at the highest flow rate, 300 L h^{-1} (C), reducing 15% of the pollutant, as shown in Fig. 4 (b).

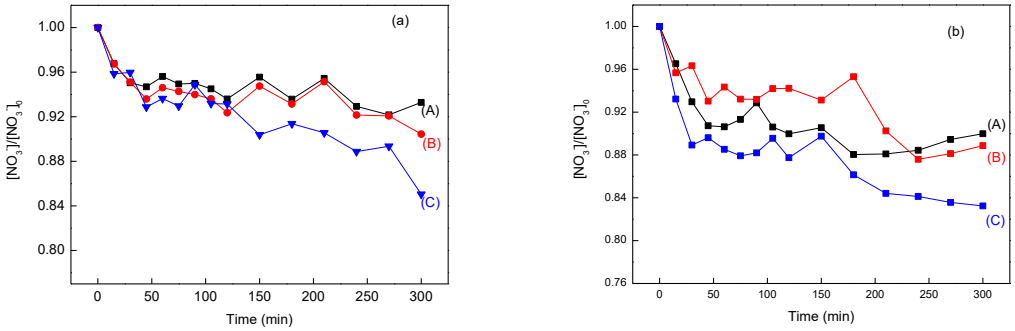

Figure 4. Nitrate removal as a function of the electrolysis time for the three flow rates of (A) 50, (B) 100, and (C) 300 L h^{-1}. (a) 20 mAcm^{-2}; (b) 200 mAcm^{-2}.

In order to justify the inference of the physical adsorption of intermediate products on the electrode surfaces, the films were analyzed by XPS before and after the degradations proving the adsorption of elements on the film surface, especially after a low flux electrolysis. Fig. 5 presents a general evaluation of the chemical composition of all elements on the BDD film surface from the XPS Survey spectra before and after the nitrate ion electrolysis process. The spectrum showed the presence of two main peaks related to C 1s (284.5 eV) and O 1s (529.2 eV) for the BDD film before nitrate ion electrolysis. As can be seen in Fig. 5, the presence of different chemical elements such as N 1s (398.6 eV), K 2p (292,8) and S 2p (164,3 eV) were observed after the nitrate ion electrolysis as possible contaminant elements on the BDD surface. Besides, the C 1s decreased associated to the O 1s peak increase, for both flow rates. These results confirm that there were adsorption of intermediates on the surface of the electrode during the process of nitrate ion reduction. Detailed information on the atomic concentrations of C 1s, O 1s, N 1s, K 2p and S 2p were calculated from the Survey spectra using Kratos Vision software. These results are presented in Table 1.

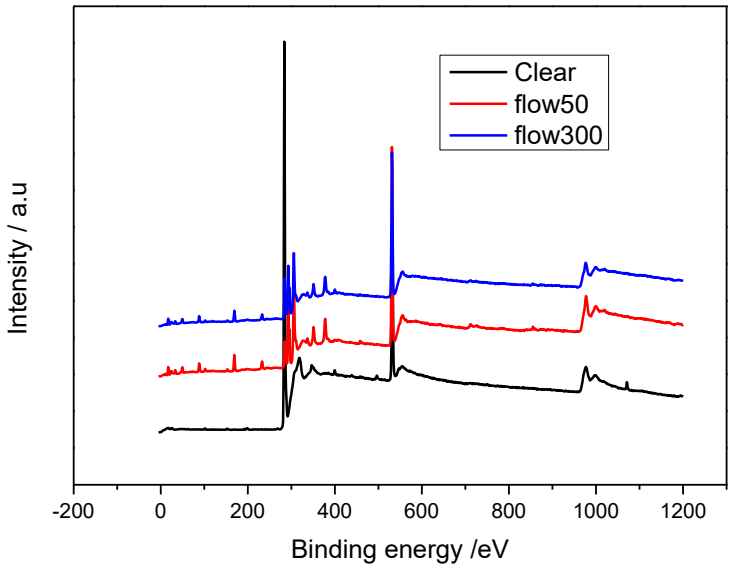

Figure 5. - XPS Survey spectra before and after the nitrate ion electrolysis process.

According to Table 1 results, there is a higher contaminant percentage when the electrolysis was performed in a 50 L h^{-1} flow ate compared to that performed with a flow rate of 300 L h^{-1}. Another significant difference is associated to the C/O ratio on the diamond surface before and after the nitrate ion reduction. There was a larger decrease in this ratio when the electrolysis was performed using a 50 L h^{-1}. This behavior may be related to a possible inhibition of active sites of the BDD electrode, as a consequence there was a small decrease in the efficiency of the reduction of the nitrate ion using flow rate of 50 L h^{-1}. It is believed that the turbulent regime, established in the higher fluxes, acts by removing the adsorbed particles in the electrode due to the great agitation generated in the displacement of the fluid by the non-linear flow rate of its particles, providing a larger contact surface between the electrode and the nitrate ion. Otherwise, the laminar regime, established in the smallest flows, presents the least agitation in the layers of the fluid during its movement, allowing particles such as hydrogen and/or intermediate products generated during the degradation to remain adsorbed on the electrode.

	Before electrolysis	After electrolysis (flow 300)	After electrolysis (flow 50)
Peak	**% mass conc.**	**% mass conc.**	**% mass conc.**
C 1s	85.13	23.92	12.07
O 1s	14.87	45.05	51.94
N 1s	-	1.11	-
K 2p	-	22.66	26.78
S 2p	-	7.19	9.09

Table 1. Mass concentration percentage of C 1s, O 1s, N 1s, K 2p, and S 2p obtained from XPS spectra

These results are coherence when compared to the degradations carried out with the current density of 20 mA cm^{-2}, confirming the tendency of the sharp drop of the pollutant concentration in the electrolysis beginning , although this behavior does not continue throughout the process. Thus, a trend was observed in the flow rate study with the use of unmodified electrodes: the higher the flow rate the better the efficiency of nitrate removal. Moreover, since a great similarity was observed between the degradations carried out in flows of 50 and 100 L h^{-1}, it was decided to neglect the study with 100 L h^{-1} in the next steps of the work based on the assumption that the small flow variation between them was not sufficient to change satisfactorily the degradation behavior.

Concerning the flow rate of 300 L h^{-1}, the rates of nitrate concentration decay are considerably different between the two applied current densities, although the final result, in degraded terms, are similar. Nonetheless, a significant drop in nitrate concentration is observed for the three initial times of collection, when the 200 mA cm^{-2} current density is used. However, this effect is greatly reduced for the lower current density. For the total degradation time the effect a current density ten times higher is not significant. By comparing the curves (C) on Fig 4 (a) and (b) results of the nitrate removal were 13 and 15% for current densities of 20 and 200 mA cm^{-2}, respectively. Although the nitrate removal was greater in the current density of 200 mA cm^{-2}, no proportionality relation was observed in comparison to that of 20 mA cm^{-2}. Therefore, the choice of 200 mA cm^{-2} is inappropriate for this study, because there is no linear relationship between the applied current density and the percentage of degraded nitrate [13]. The small increase observed in the degradation rate after a significant increase in energy expenditure may be related to the evolution reaction of hydrogen, which competes with the degradation of nitrate consuming part of the energy supplied to the electrolysis, resulting in a degradation rate of the pollutant lower than that expected [12, 13, 31, 34]. These data are in agreement with other papers where the linear relationship between energy consumption and percentage of degraded nitrate was not observed [13, 31]. In addition, these studies also confirmed that the current density of 20 mA cm^{-2} is the best choice.

Also, the specific energy consumption was performed to show that the higher current density is not appropriated according to equation 1:

$$CE = (E.I.t)/1000 \quad (1)$$

where:
E is the potential measured during the electolysis (V);
I is the applied current;
t is the electrolysis time (h).

Thus, the energy consumption may be evaluated from:

$$CEs = CE/\Delta m \quad (2)$$

where Δm is the difference between the initial and final nitrate mass during the electrolysis. These results are presented in Table 2 for the two current densities studied.

Current density (mA cm^{-2})	**Removal nitrate mass (g)**	**Potential E(V)**	**CE (kWh)**	**CEs (kWh g^{-1})**
20	$1{,}515x10^{-2}$	5,65	$7{,}063x10^{-3}$	0,466
200	$1{,}692x10^{-2}$	14,52	$1{,}836x10^{-1}$	10,85

Table 2. Relationship between the energy consumption of nitrate degradation at two current densities: 20 and 200 mA cm^{-2}.

Although the values of nitrate degraded mass are similar, the energy used in the electrolysis is totally different. In comparison, the specific energy consumption of the degradation performed using the higher current is more than twenty times greater than that of the lower current. Therefore, there is a strong dependence relation between energy consumption and current density, even if this association is not linear [35]. Taking into account that all parameters such as media resistivity, supporting electrolyte, electrodes, and flow rate were the same in the degradations, it is believed that energy excess was used in the parallel reactions of hydrogen evolution during electrolysis. In order to continue the degradations, the current density of 20 mA cm^{-2} was chosen, since it showed a more suitable relation between the consumed energy and the amount of degraded pollutant.

3.2.2. Influence of Cu/BDD/Ti cathode

After the preceding optimization parameters, the next step of this work was to apply the modified diamond films through the Cu electroless process as cathode in the electrolysis process for nitrate removal. According to Lacasa et al [14], the deposition of a thin layer of copper particles has a catalytic effect on the nitrate degradation, reducing the physical adsorption of hydrogen on the cathodic electrode surface, favoring the adsorption of the pollutant. In order to maintain a comparative parameter, the influence of the modified electrodes was studied for flow rates of 50 and 300 L h^{-1} and current density of 20 mA cm^{-2}. The comparison between the electrolysis using BDD/Ti and Cu/BDD/Ti cathodes are shown in Fig. 6 (a) and (b) for flow rates of 300 and 50 L h^{-1}, respectively.

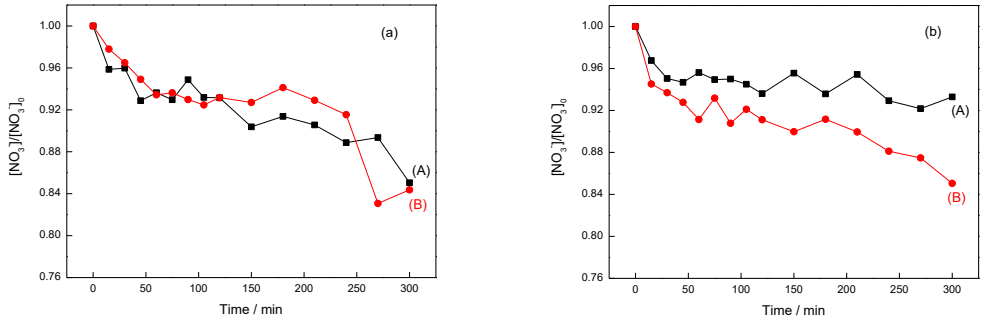

Figure 6. Nitrate removal as a function of the electrolysis time using two different cathodes of (A) BDD/Ti and (B) Cu/BDD/Ti. (a) 300 Lh^{-1}; (b) 50 L h^{-1}.

The degradation carried out with the modified cathode Cu/BDD/Ti(B) shows a slight improvement in the final value of the degradation in relation to that obtained with the cathode BDD/Ti (A). Nevertheless, the electrodes performance was similar during the electrolysis. This behavior can be attributed to the turbulent regime, which, like copper, inhibits the physical adsorption of hydrogen and/or intermediate products on the electrode surface. Nonetheless, taking into account the previous results where only BDD cathodes were used, it is important to note that the influence of flow rate variation was more significant in the electrolysis results than that for using Cu/BDD/Ti modified cathode. Similar experiments were performed for the lowest flow rate, which presented a notable behavior (Fig. 6 (b)). The laminar regime, established in the 50 L h^{-1} flow rate, generated the lowest possible stirring during the liquid flow, allowing greater physical adsorption of the substances on the electrode. Thus, in this regime, where the fluid mechanics favored the greater adsorption of particles in the films, the copper effect as catalytic metal became more expressive. While BDD/Ti (A) cathode showed a marked drop in pollutant concentration only on the end of the first hour, results using the modified Cu/DDB/Ti (B) electrode showed a more continuous decay rate throughout the process, proving the higher nitrate reduction in the lower flow. In this type of fluid flow regime copper is responsible for the lower adsorption of hydrogen in the electrodes, confirming the catalytic activity of the metal in the nitrate degradation [14, 31].

3.2.3. Influence of supporting electrolyte

The electrolysis parameter investigations showed up to now the necessity of a systematic study related to this complex process of nitrate removal. Thus, the final parameter studied is related to the supporting electrolyte influence in solution of phosphate buffer and in carbonate buffer solutions, remembering that up to this stage the medium used as supporting electrolyte was composed of K_2SO_4 0.1 mol L^{-1} and 100 ppm of KNO_3. Thus, in order to avoid conductivity discrepancies between these nitrate diluents, the ionic concentration of two media was maintained at 0.1 mol L^{-1}. Also, the initial pH = 7 of phosphate buffer solution was the same to that of sulfate medium, while for carbonate buffer solution the pH = 10. The current density was kept at 20 mA cm^{-2} for a flow rate of 50 L h^{-1}. The electrolysis results are depicted in Fig. 7. The first medium studied was sulfate (A). Comparatively, this medium showed the greatest drop in the pollutant concentration in the first 50 min of electrolysis. In this range, the carbonate buffer (B) showed the lowest drop while the phosphate buffer solution (C)

had an intermediate behavior. On the other hand, analyzing the final degradation, the phosphate buffer solution had the best result, followed by the sulfate solution while the carbonate buffer was the supporting electrolyte with the lowest degradation, very close to that for sulfate electrolyte.

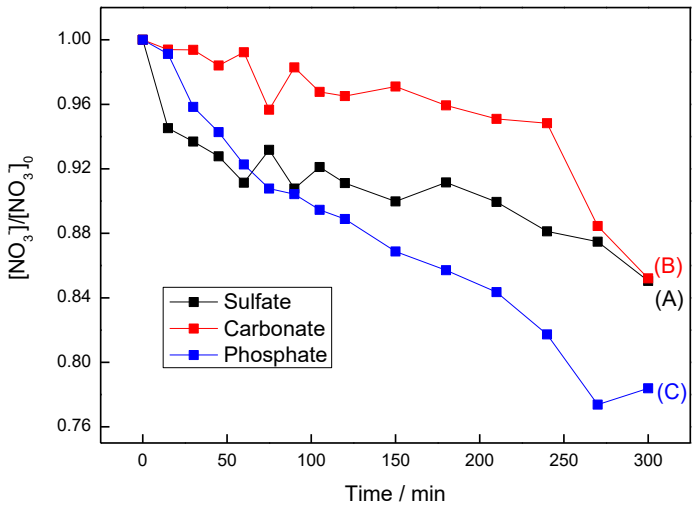

Figure 7. Nitrate removal for different supporting electrolytes at 20 mA cm^{-2} and 50 L h^{-1} using Cu/BDD/Ti as cathode. (A) potassium sulfate; (B) carbonate buffer solution; (C) Phosphate buffer solution.

In terms of energy spending, there was a small increase in consumption when the carbonate buffer solution was used in relation to that of sulfate. The latter demonstrated the best relationship between degraded mass and energy consumption. The sulphate solution further degraded comparatively the largest amount of nitrate mass, and was able to maintain the specific energy consumption in level comparable to that for other supporting electrolytes, according to Table 3.

Supporting electrolyte	**Removal nitrate mass (g)**	**Potential E(V)**	**CE (kWh)**	**CEs (kWh g^{-1})**
Sulfate	$1.514x10^{-2}$	5.43	$6.787x10^{-3}$	0.448
Carbonate	$1.493x10^{-2}$	5.97	$7.462x10^{-3}$	0.499
Phosphate	$2.185x10^{-2}$	8.66	$10.83x10^{-3}$	0.495

Table 3. Relationship among the energy consumption of nitrate degradation in three support electrolyte of sulfate, carbonate buffer, and phosphate buffer.

The use of carbonate buffer solution resulted in an increase in energy consumption relative to that of sulfate resulting in its lowest nitrate reduction in terms

of degraded mass. Also, phosphate buffer solution demonstrated an energy spending comparable to that of carbonate buffer solution. Nonetheless, this was the supporting electrolyte that presented the greatest nitrate degradation.

Conclusion

In summary, some parameters of the electrochemical flow reactor were optimized in the study of nitrate electrolysis using BDD/Ti and/or Cu/BDD/Ti as cathode material. A small increase in electrolysis efficiency was obtained for BDD/Ti in highest flow rate of 300 L h^{-1} due to the lower adsorption of impurities at the electrode surface, attributed to the turbulent reactor regime. On the other hand, using Cu/BDD/Ti electrodes in the cathodic region, better results were observed in the lowest flow rate studied, which may be associated to the lower hydrogen and/or intermediate products adsorption process in the electrode promoted by Cu. The current density of 20 mA cm^{-2} was the most appropriate because no linearity relationship was observed between the increase in applied current density and the percentage of degraded nitrate. Among the evaluated media, the phosphate buffer degraded more polluting with a proportional lower energy expenditure.

References

[1] Falkenberg LJ, Stian CA. Too much data is never enough: A review of the mismatch between scales of water quality data collection and reporting from recent marine dredging programmes. Ecological Indicators. 2014; 45: 529-537.

[2] Szabo J, Minamyer S. Decontamination of biological agents from drinking water infrastructure: A literature review and summary. Environment International. 2014; 72: 124-128.

[3] Baird C, CANN M. Química Ambiental. Bookman, Porto Alegre; 2011.

[4] Rajic Lj, Berroa D, Gregor S, Elbakri S, MacNeil M, Alshawabkeh AN. Electrochemically-induced Reduction of Nitrate in Aqueous Solution. International Journal of Electrochemical Science. 2017; 12: 5998 – 6009.

[5] Glade MJ. Food, nutrition, and the prevention of cancer: a global perspective. American Institute for Cancer Research/World Cancer Research Fund, American Institute for Cancer Research, 1997. Nutrition. 1999; 15(6): 523-6.

[6] Sisinno CLS. Non-inert industrial solid waste disposal in landfill dumps: evaluation of toxicity and implications for the environment and human health. Caderno de Saúde Pública. 2003; 19 (2): 369-374.

[7] Rego Filho MTN, Braga ACR, Curi CR. A dimensão da disponibilidade hídrica: uma análise entre a conjuntura brasileira e o relatório de desenvolvimento mundial da água. Ambiência. 2014; 10 (1):111-124.

[8] Winkler M, Coats ER, Brinkman CK. Advancing post-anoxic denitrification for biological nutrient removal. Water Research. 2011; 45: 6119-6130.

[9] Kalaruban M, Loganathan P, Shim WG, Kandasamy J, Naidu G, Nguyen TV, Vigneswaran S. Removing nitrate from water using iron-modified Dowex 21K XLT ion exchange resin: batch and fluidised-bed adsorption studies. Separation and Purification Technology. 2016; 158: 62-70.

[10] Epsztein R, Nir O, Lahav O, Green M. Selective nitrate removal from groundwater using a hybrid nanofiltration-reverse osmosis filtration scheme. Chemical Engineering Journal. 2015; 279: 372-378.

[11] Thomas JM, Thomas JW. Principles and practice of heteregenous catalysis. Wheinhein, New York; 1997.

[12] Reyter D, Bélanger D, Roué L. Nitrate removal by a paired electrolysis on copper and Ti/IrO2 coupled electrodes - influence of the anode/cathode surface area ratio. Water Research. 2010; 44: 1918-1926.

[13] Li M, Feng C, Zhang Z, Yang S, Sugiura N. Treatment of nitrate contaminated water using an electrochemical method. Bioresource Technology. 2010; 101: 6553-6557.

[14] Lacasa E, Cañizares P, Llanos J, Rodrigo MA. Effect of the cathode material on the removal of nitrates by electrolysis in non-chloride media. Journal of Hazardous Materials. 2012; 213-214: 478-484.

[15] Lacasa E, Cañizares P, Llanos J, Rodrigo MA. Electrochermical denitrification with chlorides using DSA and BDD anodes. Chemical Engineering Journal. 2012; 184: 66-71.

[16] Yang J, Sebastian P, Duca M, Hoogenbooma T, Koper MTM. pH dependence of the electroreduction of nitrate on Rh and Pt polycrystalline electrodes. Chemical Communication. 2014; 50: 2148-2151.

[17] Estudillo-Wong LA, Arce-Estrada EM, Alonso-Vante N, Manzo-Robledo A. Electro-reduction of nitrate species on Pt-based nanoparticles: surface area effect. Catalysis Today. 2011; 166: 201-204.

[18] Wang Q, Zhao X, Zhang J, Zhang X. Investigation of nitrate reduction on polycrystalline Pt nanoparticles with controlled crystal plane. Journal Electroanalytical Chemistry. 2015; 755:210-214.

[19] Su JF, Ruzybayev I, Shah I, Huang CP. The electrochemical reduction of nitrate over micro-architectured metal electrodes with stainless steel scaffold. Applied Catalysis B: Environmental. 2016; 180: 199-209.

[20] Katsounaros I, Kyriacou G. Influence of nitrate concentration on its electrochemical reduction on tin cathode: identification of reaction intermediates. Electrochimica Acta. 2008; 53: 5477-5484.

[21] Pérez G, Ibáñez R, Urtiaga AM, Ortiz I. Kinetic study of the simultaneous electrochemical removal of aqueous nitrogen compounds using BDD electrodes. Chemical Engineering Journal. 2012; 197: 475–482.

[22] Reuben C, Galun E, Cohen H, Tenne R, Kalish R, Muraki Y, Hashimoto K, Fujishima A, Butler JM, Lévy-Clément, C. Efficient reduction of nitrite and nitrate to ammonia using thin-film B-doped diamond electrodes. Journal Electroanalytical Chemistry. 1995; 396: 233–239.

[23] Ndao AN, Zenia F, Deneuville A, Bernard M, Lévy-Clément C. Effect of boron concentration on the electrochemical reduction of nitrates on polycrystalline diamond electrodes. Diamond Related Materials. 2000; 9: 1175–1180.

[24] Matsushima JT, Silva WM, Azevedo AF, Baldan MR, Ferreira NG. The influence of boron content on electroanalytical detection of nitrate using BDD electrodes. Applied. Surface Science. 2009; 256: 757–762.

[25] Lévy-Clément C, Ndao NA, Katty A, Bernard M, Deneuville A, Comninellis C, Fujishima A. Boron doped diamond electrodes for nitrate elimination in concentrated wastewater, Diamond Related Materials. 2003; 12: 606–612.

[26] Govindan K, Noela M, Mohan R. Removal of nitrate ion from water by electrochemical approaches. Journal of Water Process Engineering. 2015; 6: 58–63.

[27] Couto AB, Oishi SS, Ferreira NG. Enhancement of nitrate electroreduction using BDD anode and metal modified carbon fiber cathode. Journal of Industrial and Engineering Chemistry. 2016; 39: 210-217.

[28] Ghazouani M, Akrout H, Bousselmi L. Efficiency of electrochemical denitrification using electrolysis cell containingBDD electrode. Desalination and Water Treatment. 2014; 53: 1-11.

[29] Pereira CF, Couto AB, Baldan MR, Ferreira NG. Copper Electroless Process Optimization to Modify Boron Doped Diamond at Different Boron Levels. ECS Transactions. 2015; 64: 15-22.

[30] Forti JC, Rocha RS, Lanza MRV, Bertazzoli R. Electrochemical synthesis of hydrogen peroxide on oxygen-fed graphite/PTFE electrodes modified by 2-ethylanthraquinone. Journal of Electroanalytical Chemistry. 2007; 601: 63–67.

[31] Ribeiro MCE, Couto AB, Ferreira NG, Baldan MR. Nitrate Removal by Electrolysis Using Cu/BDD Electrode Cathode. ECS Transactions. 2014; 58: 21-26.

[32] Hasnat MA, Agui R, Hinokuma S, Yamaguchi T, Machida M. Different reaction routes in electrocatalytic nitrate/nitrite reduction using an H+- conducting solid polymer electrolyte. Catalysis Communications. 2009; 10: 1132-1135.

[33] Hasnat MA, Amirul Islam M, Borhanuddin SM, Ullah Chowdhury MR, Machida M. Influence of Rh on electrocatalytic reduction of NO3- and NO2- over Pt and Pd films. Journal of Molecular Catalysis A: Chemical. 2010; 317: 61-67.

[34] Szpyrkowicz L, Daniele S, Radaelli M, Specchia S. Removal of NO3- from water by electrochemical reduction in different reactor configurations. Environmental. 2006; 66: 40-50.

[35] Katsounaros I, Dortsiou M, Kyriacou G. Electrochemical reduction of nitrate and nitrite in simulated liquid nuclear wastes. Journal of Hazardous Materials. 2009; 171: 323-327.